# *Staphylococcus aureus* prophages are gatekeepers of lipid utilization to control membrane flexibility, bacterial fitness, and antibiotic adaptation

Byang Zhou[a], Amit Pathania[a], Deepak Pant[a], David Halpern[a] Philippe Gaudu[a], Patrick Trieu-Cuot[b], Alexandra Gruss[a] and Karine Gloux[a].

[a]Université Paris-Saclay, INRAE, AgroParisTech, Micalis Institute, Jouy en Josas, France,

[b] Institut Pasteur, Université de Paris, CNRS UMR 2001, Unité de Biologie des Bactéries Pathogènes à Gram-Positif, Paris Cedex 15, France.

For correspondence: karine.gloux@inrae.fr

Key words: triglycerides, diglycerides, sphingomyelins, FASII, bacteriophage, Geh lipase, Hlb hemolysin B, FakB1, FASII antibiotics.

## Importance

*Staphylococcus aureus* is a major human health challenge. Its lipases are crucial for virulence and immune response escape. Prophages inserted in lipases are common in *S. aureus* but the selective benefits of their maintenance is little understood. We demonstrate that two prophages, inserted in triglyceride and sphingomyelin lipase genes, interactively modulate fatty acid incorporation into bacterial membranes. The presence or absence of prophage determine how bacteria respond to a complex lipid environment such as the host, by affecting membrane properties, fitness, and adaptation to antibiotics inhibiting fatty acid synthesis. Our findings highlight the importance of assessing prophage status and lipid environments when evaluating infection risk and therapy efficiency.

## Abstract

Lipids are essential components of bacterial membranes and phages are quasi-ubiquitous in bacteria. Both are crucial mediators of bacteria-host interactions. In the major pathogen *Staphylococcus aureus*, two common prophages, ϕ11.1 and ϕ13, are preferentially integrated in lipase genes, respectively encoding Geh, a triglyceride lipase, and Hlb, a sphingomyelinase. Here we report how prophage status, and consequently lipase availability, impacts *S. aureus* metabolism of environmental lipids, and overall bacterial fitness. The fatty acid kinase subunit FakB1, known to promote saturated fatty acid incorporation, also facilitates incorporation of unsaturated fatty acids released from triglycerides by Geh; this process occurs only when ϕ11.1 is absent. Geh and Hlb lipase products compete for FakB1, and interference by prophage integration changes the outcome of this competition. Our findings could explain the selective advantage of prophage conservation, as a means of modulating bacterial membrane composition and preventing toxicity of environmental lipids. ϕ13 lysogeny also impaired the bacterial capacity to escape antibiotic inhibitors of FASII (fatty acid synthesis). We suggest that testing new therapeutics against *S. aureus* should consider prophage status and environmental lipids for accurate prediction of efficiency.

## Introduction

Environmental lipids comprise an integral, but often overlooked, aspect of bacterial pathogenesis. Lipids are crucial for bacterial fitness and are front-line players in modulating interactions with the host (1-4). Lipids range in structure from simple short hydrocarbon chains to complex molecules, including triglycerides (TGs), phospholipids (PLs), sterols and their esters.

48 Fatty acids (FA), the basic constituents of complex lipids, vary in chain length, side chains, and
49 number and position of double bonds. A vast array of bacteria scavenge FA, which they
50 incorporate into their membranes (5-11). This quasi-ubiquity suggests a great potential of the
51 host lipid environment to modulate invading pathogen behavior. The environmental lipid
52 composition depends on human genetics and diet and is correlated to infection risk (12, 13, 3,
53 4). *Staphylococcus* aureus, a major human pathogen, incorporates exogenous FA, such as those
54 present in plasma lipids (14, 9). Incorporation involves a FA kinase, FakA, whose preference for
55 saturated and unsaturated FA is reportedly respectively conferred by the FA binding proteins
56 FakB1 and FakB2 (15-17). While *S. aureus* does not synthesize unsaturated and polyunsaturated
57 FA (UFA and PUFA), their incorporation has documented effects on bacterial membrane
58 functions and interactions with the host (18-22).

59 Prophages are potent factors of virulence, as reported in *S. aureus* (23). Remarkably, two
60 commonly found *S. aureus* prophages, ϕ11-1 and ϕ13, are inserted in *geh* and *hlb* genes
61 encoding lipases, respectively Geh glycerol ester hydrolase (EC 3.1.1.3) and Hlb neutral
62 sphingomyelinase C (EC 3.1.4.12) (24, 25) (Fig. 1A). About 15% of *S. aureus* isolates carry ϕ11.1
63 in *geh* and at least 90% of human clinical isolates carry ϕ13 in *hlb* (1, 26). In contrast ϕ13
64 prophage was quasi-absent in livestock isolates. ϕ11-1 and ϕ13 prophage excision is induced by
65 environmental signals (such as SOS response or biocide/$H_2O_2$ respectively), leading to
66 reactivation of Geh and Hlb activities with consequent impacts on *in vivo* inflammatory responses
67 (1, 27-31, 23). In contrast consequences of lipase genes inactivation by ϕ11.1 and ϕ13 on *S.*
68 *aureus* metabolism and physiology have been little explored (14). Here we show that these two
69 widespread prophages interactively affect membrane phospholipid composition and growth
70 response to toxic UFA C18:2. The FA binding protein FakB1 is identified as a control point for
71 phage-dependent dynamic competition between FA issued from triglycerides and

72 sphingomyelins. Finally, ϕ13 lysogeny led to impaired efficiency of anti-FASII antibiotics
73 compared to non-lysogens, further underlining the importance of prophage in *S. aureus* fitness.

74

75 **Results**

76 **ϕ13 lysogeny increases C18:2 incorporation from serum into *S. aureus* phospholipids.** We
77 analyzed FA profiles from two isogenic Newman strains (WT and Δϕ13), which differ by the
78 presence of ϕ13 prophage (19). The ϕ13-lysogenized WT and Δϕ13 strains showed identical FA
79 profiles in control BHI medium,, indicating that FASII-synthesis was unaffected by ϕ13 (Fig. S1).
80 In contrast, addition of 10% mouse serum to medium distinguished the two strains by their
81 incorporation of UFA. The Δ ϕ13 strain had approximately two times less UFA than the WT (6 ±
82 1% *versus* 13 ± 1%), including oleic acids C18:1Δ9, C18:1Δ11, and the PUFA linoleic acid C18:2
83 (Fig. 1B). Serum was the only UFA source for *S. aureus*, which lacks UFA synthesis and desaturase
84 functions (32). These results thus suggested an unexpected link between ϕ13 lysogenic status
85 and UFA incorporation from a serum source.

86 **ϕ11.1 lysogeny decreases trilinolein-derived C18:2 incorporation, elongation and toxicity; ϕ13**
87 **effects depend on ϕ11.1 status**. Trilinolein (TNL), a TG with three C18:2, is a substrate for Geh
88 lipase (33). We asked how the *geh/*ϕ11.1 status impacts breakdown of TNL to C18:2, and whether
89 ϕ13 lysogeny affects this process. For this, we analyzed FA profiles of isogenic Newman strains
90 lysogenized or not with ϕ11 (including the three ϕ11.1 to ϕ11.3 prophages) and ϕ13 prophages
91 (19). In BHI medium, the ϕ11 prophage status had no detectable effect on FA profiles which
92 reflect endogenous FA synthesis (Fig. S1). In contrast, TNL addition led to marked differences in
93 FA profiles and growth: the ϕ11 lysogenized strains showed markedly less C18:2 incorporation
94 from TNL and improved growth compared to non- ϕ11 lysogens (Fig. 1C). This result is in

95 accordance with *geh* inactivation by ϕ11.1 and C18:2 toxicity on *S. aureus* (34). The remaining
96 18:2 incorporation in the ϕ11 lysogens may indicate residual Geh activity despite the C-terminal
97 truncation, or C18:2 release by other lipases. Strikingly, ϕ11 lysogeny correlated with a quasi-
98 total inhibition of C18:2 elongation by FASII (Fig. 1C) suggesting that Geh facilitates accessibility
99 of TNL-derived C18:2 to FASII pathway. Furthermore, the ϕ13 lysogeny had effects depending on
100 the ϕ11 status. Indeed when ϕ11.1 was present, ϕ13 lysogeny led to higher C18:2 incorporation
101 from TNL (11 ± 1% in WT *versus* 4 ± 0.5% in Δϕ13 strain). In contrast, in absence of ϕ11.1 (intact
102 *geh*), it did not impact the C18:2 incorporation (28 ± 4% in Δϕ11 *versus* 28 ± 1% in Δϕ11Δϕ13
103 strain, Fig. 1C) but increases elongation of both C18:2 (from 50 to 70%) and C20:2 (from 14 to
104 28%). These observations point to an unexpected interconnection between *S. aureus* ϕ11 and
105 ϕ13 prophages for both incorporation and elongation of the PUFA C18:2 from TNL.

106 **A *geh* mutant shows decreased incorporation of trilinolein-derived C18:2 and its elongation.**
107 We asked whether ϕ11 prophage family effects were due to *geh* gene interruption by ϕ11.1. We
108 analyzed the strain USA300 which lacks ϕ11.1 (intact *geh*) and its isogenic *geh::tn* mutant. While
109 TNL-derived C18:2 was incorporated and efficiently elongated in both these strains,
110 incorporation and particularly elongation were markedly lowered in the USA300 *geh::tn* mutant
111 (Fig. 1D). Both *geh*::tn mutant and ϕ11 Newman lysogens encode C-terminal truncations of Geh
112 (at respective amino acid [aa] positions 517 and 643 from a full length protein of 690 aa).
113 Furthermore, orlistat, an inhibitor which binds to Geh (35), inhibited both incorporation and
114 elongation of C18:2 from TNL (Fig. 1D). These results indicate that the Geh state, rather than an
115 intrinsic property of ϕ11.1, determines *S. aureus* capacity to both incorporate and elongate TNL-
116 derived C18:2.

117 **1,3-diglyceride-derived C18:2 is efficiently incorporated and toxic for growth.** In TGs, the UFA
118 position on the glycerol backbone affects its absorption and metabolism by cells (36-38).
119 Triglyceride lipases display positional selectivity, which can be discriminated using 1,2-
120 dilinoleoylglycerol (1.2DG) and 1,3-dilinoleoylglycerol (1.3DG) as substrates (39-41). Geh
121 reportedly cleaves TNL in both positions 1 and 2 whereas most lipases prefer position 1 (39, 40).
122 Consequently, Geh activity liberates 1.3DG from TNL, in contrast to other lipases. We therefore
123 examined C18:2 incorporation from 1.2DG and 1.3DG in WT, Δϕ11, Δϕ13 and Δϕ11Δϕ13
124 Newman isogenic strains. Addition of 30 µM 1.2DG led to low-level C18:2 incorporation whatever
125 the prophage status. A growth retardation was observed in the Geh$^+$ strains (non-ϕ11.1 lysogens)
126 where both incorporation and elongation were favored (Fig. 1E). The same concentration of
127 1.3DG lead to lysis of non-ϕ11.1 lysogens (data not shown). Lowering 1.3DG addition to 10 µM
128 avoided lysis. Under this condition, very high incorporation and elongation of C18:2 clearly
129 occurred only when Geh is intact (in non-ϕ11.1 lysogens). TG hydrolysis product, particularly
130 attributed to Geh activity, leads therefore to high PUFA incorporation and elongation in *S. aureus*.

131 **Serum-derived C16 incorporation is increased in Δϕ13 and *hlb*$^+$ strains.** We focused on possible
132 mechanisms involved in ϕ13 impact on UFA incorporation. In the presence of 10% mouse serum,
133 the percentage of C16 and its derived FA (C18 + C20) was decreased in Newman WT strain
134 compared to the Δϕ13 strain in favor of incorporated serum UFA (Fig. 2A). Serum sphingomyelins
135 are dominant circulating Hlb substrates that contain mainly C16 as FA moieties (42, 43). To
136 further understand how *hlb* affects UFA utilization, we complemented the USA300 *hlb::tn* mutant
137 with a plasmid carrying an intact *hlb* gene. Hlb complementation increased C16 and elongated
138 derived FA whereas it decreased incorporated serum UFA (Fig. 2B). These results indicate that
139 *hlb* contributes to C16 liberation and its further incorporation whereas ϕ13 lysogeny increases

140 serum UFA incorporation. Based on these observations, we hypothesized that the ϕ13
141 lysogenic/excised status likely creates a dynamic competition between C16 and UFA from serum
142 TGs for incorporation in membrane phospholipids.

143 **Incorporation of 1.3DG-derived C18:2 requires *fakB1*.** The FakA kinase preference for saturated
144 and unsaturated FA incorporation is reportedly conferred by FakB1 and FakB2, respectively (15-
145 17). We first confirmed the reported phenotypes in USA300 derivative *fakA*, *fakB1*, and *fakB2*
146 mutants in keeping with a minor role of FakB1 in UFA incorporation, including that of free C18:2
147 PUFA (Fig. S2 and S3)(16, 17)). We then challenged USA300 derivative *fakA*, *fakB1*, and *fakB2*
148 mutants with TNL. The *fakA* mutant failed to incorporate TNL-derived C18:2 (data not shown).
149 Unexpectedly, *fakB1* and *fakB2* mutants failed to show selectivity when TNL was used as C18:2
150 precursor; both mutants displayed the capacity to incorporate C18:2 from TNL (Fig. S4). Thus,
151 while free C18:2 incorporation was FakB2-dependent (see Fig. S3), incorporation from TNL-
152 derived C18:2 was permissive. The strong effects of 1.3DG on non-ϕ11.1 lysogens growth and on
153 C18:2 incorporation, compared to 1.2DG (Fig. 2), led us to examine incorporation of these
154 substrates in *fakA*, *fakB1*, and *fakB2* backgrounds. *fakA* was essential for incorporation of both
155 substrates, reflecting the phosphorylation requirement ((17); data not shown). Incorporation of
156 1.2DG-derived C18:2 was in accordance with the reported FakB2 binding phenotype (15-17) (Fig.
157 S5). In contrast, incorporation of 1.3DG-derived C18:2 was remarkably greater in *fakB2* than in
158 *fakB1* mutant (20 ± 7% versus 13 ± 3%) and *fakB1* inactivation results in markedly lower
159 incorporation compared to the USA300 wild type (13 ± 3 % and 31 ± 5% respectively, Fig. 3A).

160 To confirm the direct role of *fakB1*, we used RN450 strain, cured of phage lysogens and with a
161 natural *fakB1* in-frame deletion (483-bp within the 867-bp functional gene, Fig. S6) and the
162 isogenic RN450-R strain, repaired for *fakB1*. The RN450-R repaired strain incorporated more

163 1.3DG-derived C18:2 than RN450 strain (35 ± 3% and 27± 3% respectively, Fig. 4A). Furthermore
164 1.3DG impairs more growth of *fakB1* defective strains (the USA300 *fakB1* mutant and RN450
165 strain) compared to their respective *fakB1*$^{+}$ controls (WT USA300 and RN450-R, Fig. 3; Fig. 4).
166 These observations identified therefore FakB1 binding as the unconventional preferred pathway
167 for efficient incorporation of 1.3DG-derived C18:2 into PL and as a contributor of growth
168 protection.

169 **1,3-diglyceride-derived C18:2 and C16 compete for FakB1.** The unexpected role of FakB1 in
170 C18:2 incorporation from tri- and di-glycerides (Fig. S4A, 3A, 4A) led us to ask whether C16,
171 favored in *hlb*$^{+}$ strains, competes for FakB1. To test this, C16 was also added in experiments
172 discussed above. We first established that, as reported, free C16 and free C18:2 were poorly
173 competitive ((16), Fig. S3). In the *fakB1* background (USA300 WT and *fakB2* mutant), addition of
174 free C16 led to a slight decrease in C18:2 incorporation from either TNL or 1.3DG (Fig. S4, Fig 3).
175 The 1.3DG-derived C18:2 incorporation is little affected in the WT (22 ± 1 % compared to 31 ±
176 5%) and unaffected in the *fakB1* mutant (14 ± 4 % compared to 13 ± 3%). In contrast, when only
177 FakB1 is available (in the *fakB2* mutant), C16 addition led to a quasi-total arrest of C18:2
178 incorporation (Fig. S4, Fig 3). As example, *fakb2* mutant has more than three times less 1.3DG-
179 derived C18:2 in the presence of C16 (6 ± 3% compared to 20 ± 7%). In RN450 (naturally fakB1
180 defective), *fakB2* can compensate for C18:2 incorporation from 1.3DG but C16 had no
181 competitive effect (Fig. 4). A direct role for *fakB1* was confirmed using RN450-R, repaired for
182 *fakB1.* Notably, total incorporation of 1.3DG-derived C18:2 is highly increased in this strain and
183 quasi-totally inhibited (80 ± 10% decreased) in the presence of free C16 (Fig. 4). FakB1 is
184 therefore a key determinant responsible for competition between C16 and 1.3DG-derived C18:2.

185

186 **ϕ13 lysogeny delays *S. aureus* adaptation to FASII antibiotics.** We showed previously that *S.*
187 *aureus* can overcome inhibition by FASII antibiotics by incorporating exogenous FA (9) . We
188 reasoned that ϕ13 and/or ϕ11 lysogeny might affect this process, as lipase activity might be
189 needed to first liberate FA. Anti-FASII adaptation of *S. aureus* lysogens and non-lysogens was
190 therefore compared in medium containing mouse serum, using the FabI- antibiotic AFN-1252
191 (44). Remarkably, the absence of ϕ13, but not ϕ11.1, resulted in faster *S. aureus* outgrowth during
192 anti-FASII adaptation using two different antimicrobials, AFN-1252 (Fig. 5)) and triclosan (data
193 not shown). This observationsuggests that restoring Hlb lipase may improve *S. aureus* access to
194 exogenous lipids, thereby facilitating bypass of the FASII-antibiotic block.

195 **Discussion**

196 *S. aureus* metabolism of environmental lipids is modulated by two common prophages, ϕ11.1
197 and ϕ13, which interrupt the lipases encoding genes *geh* and *hlb*. The present work reveals
198 expanded roles for these prophages on exogenous lipid utilization and bacterial fitness. Three
199 interactive factors determine the bacterial responses: the environmental lipid offer, which is
200 highly variable according to the biotope; the status of prophages, which toggle the lipase genes
201 and control FA content and elongation in membrane phospholipids; and the FA kinase FakB1,
202 which controls competitive entry of PUFA and saturated FA released from lipids. Our work
203 demonstrates that lysogeny by ϕ11.1 and ϕ13 protects bacteria from lipid toxicity and modulates
204 membrane flexibility, thus conferring a selective benefit for prophage maintenance.

205 We propose a model for a two-level control of FA incorporation and elongation, first by
206 prophages, and then by FakB1 (Fig. 6).

207 The first control is determined by ϕ11.1 lysogeny, which protects *S. aureus* from PUFA toxicity.
208 When TG is available, ϕ11.1 lysogens carrying truncated Geh show decreased PUFA C18:2
209 incorporation and limited elongation compared to non-ϕ11.1 lysogens. To our knowledge this is
210 the first report that Geh impacts FASII elongation efficiency. PUFA provoke membrane
211 permeabilization and lysis (45-50). Unlike most lipases, Geh cleavage of TG liberates both 1,2-
212 and 1,3-diglycerides (39, 40); direct 1.3DG addition led to greater toxicity than did 1.2DG. By
213 inactivating Geh, ϕ11.1 lysogeny exerts a protective role on *S. aureus* by limiting PUFA release
214 and incorporation in membrane phospholipids, and likely improves bacterial survival in natural
215 lipid-rich environments. Considering ϕ13 lysogeny, its prevalence among human clinical *S. aureus*
216 isolates (26) suggests a functional benefit of preventing Hlb activity. As expected, *hlb,* intact in
217 the absence of ϕ13, led to increased saturated FA incorporation from serum. Remarkably
218 however, intact *hlb*, which is not implicated in PUFA metabolism, also reduced PUFA
219 incorporation and elongation.

220 FakB1 defines the second level of control. While FakB1 is reportedly associated with saturated
221 FA binding (15-17), it also mediates efficient incorporation of C18:2 issued from 1.3DG cleavage
222 by Geh. Entry of 1.3DG -derived C18:2 contrasts with both free and 1.2DG-derived C18:2, which
223 involves mainly FakB2. Thus FakB1 binding is more permissive than initially reported, in
224 accordance with recent studies (16, 51, 17). We propose that FakB1 acts as a C18:2 chaperone
225 that prevents cytoplasmic toxicity (34), prior to membrane incorporation. FakB1-C18:2 binding
226 would lead to FakA-mediated C18:2 phosphorylation of FA, which is required for FA efflux, and
227 hence bacterial protection, *via* FarE (52). Further investigation will elucidate the TG intermediate
228 recognized by FakB1, and the contributions of Geh to these binding specificities.

229 The unexpected role of FakB1 in PUFA incorporation reveals a new role of Hlb as generating
230 interference with unsaturated FA incorporation. Hlb activity in ϕ13 non-lysogens increases entry
231 of saturated FA, that binds FakB1, and compete with PUFA. FakB1 is thus a gatekeeper that
232 selects between PUFA and saturated FA for incorporation in membrane phospholipids. If PUFA-
233 FakB1 binding is out-competed by saturated FA, the free intracellular PUFA would not be
234 phosphorylated and effluxed, thus compromising *S. aureus* survival.

235 We propose that the combined effects of prophages and FakB1 on FA incorporation are relevant
236 to *S. aureus* infection. Both ϕ11.1 and ϕ13 phage may be maintained episomally and reintegrated,
237 implying transient activation of *geh* and *hlb* expression (53, 26, 27, 29-31, 23); these events may
238 help adjust bacterial membrane lipids during infection. PUFA may in turn impact the life cycle of
239 these prophages.

240 The composition and levels of TGs and SMs vary among individuals according to their state of
241 health and dietary intake. These factors are determinants of infection risk and predisposition to
242 bacterial resistance (54-56, 43, 57, 58). TGs are major reservoirs of long chain UFA and PUFA
243 liberated by Geh activity and incorporation of these FA alters bacterial membrane functions and
244 host interactions (18, 21, 9, 59, 22). Cholesterol was recently reported to be a Geh substrate (21),
245 suggesting another lipid substrate that might impact *S. aureus* fitness according to prophage.
246 Interestingly, intact Geh contributes to masking *S. aureus* from immune surveillance by the TLR2
247 receptor (1, 60) and 1,2-diglycerol moieties are involved in the interaction TLR2 (61). Roles of
248 Geh-mediated position 2 hydrolysis and ϕ11.1 lysogeny on immune escape merit further
249 investigation.

250 The *in vivo* significance of ϕ13 impacts on PUFA incorporation and elongation is intriguing. ϕ13
251 maintenance in the *hlb* locus or integration into atypical sites was observed in non human

252 mammals or in cystic fibrosis disease (26, 62). Differences in the lipid environments in these cases
253 may select for prophage excision from its preferred site. Interestingly, *S. aureus* escape from anti-
254 FASII inhibition in the presence of serum was facilitated in strains carrying intact *hlb*. While the
255 mechanisms underlying more efficient bacterial adaptation to anti-FASII antibiotics remain to be
256 elucidated, a simple explanation would be an increased access to environmental FA, which
257 compensate the FASII block. In accordance our model (Fig. 6), saturated FA liberated from serum
258 sphingomyelin may protect *S. aureus* from lysis due to membrane incorporation of serum PUFA
259 and thus reduces latency before adaptation. These results illustrate how prophage status can
260 impact antimicrobial resistance, and should be considered when conducting antimicrobial
261 screenings.

262 In conclusion, ϕ11.1 and ϕ13 are interactive regulators of *S. aureus* membrane phospholipid
263 composition in response to environmental TGs and SMs. Our findings lead us to suggest that
264 prophage lysogeny contributes to protecting bacteria from lipid toxicity. Prophage instability also
265 offers greater membrane flexibility, which contributes to *S. aureus* adaptation in different host
266 biotopes. While Hlb (ß toxin) is an *S. aureus* virulence factor, we showed that it affects bacterial
267 fitness in response to environmental triglycerides. Thus, by controlling FA availability from
268 triglycerides and sphingomyelins, ϕ11.1 and ϕ13 exert a fine tuning between metabolism of
269 lipids and their toxicity. These results provide new mechanistic insights of *S. aureus* lipid
270 physiology and indicate the need to assess mechanisms of prophage/lipase switches in
271 developing strategies against *S. aureus* infection.

272

273 **Materials and methods**

274 **Bacterial strains.** *S. aureus* Newman, USA300 FPR3757 JE2 (called here USA300), and NCTC 8325
275 derivative strains RN450 and RN450-R, were used in this study. Isogenic Newman strains
276 differentiated by the presence of prophages were provided by Dr O. Schneewind (Department of
277 Microbiology, University of Chicago). Newman strain has 4 prophages which are from
278 Siphoviridae family: ϕ11.1, ϕ11.2 and ϕ11.3 from Sfi 11/Sa6 subfamily and ϕ13 from Sfi 21/Sa3
279 subfamily (24). Methicillin-resistant USA300 and the Nebraska library of transposon insertions
280 (University of Nebraska Medical Center) were generously supplied by BEI resources (63). USA300
281 derivatives from this library used in this work contained insertions in the following genes:
282 SAUSA300_0320 (*geh*), SAUSA300_1973 (*hlb*), SAUSA300_1119 (*fakA*), SAUSA300_0733 (*fakB1*),
283 SAUSA300_1318 (*fakB2*); all mutants were verified by PCR. RN450 is a phage-free derivative of
284 the NCTC 8325 strain (64). It was repaired for a natural *fakB1* deletion as described for another
285 strain (65).

286 **Construction of *hlb* complemented strain.** A PCR fragment containing the *S. aureus* subsp.
287 *aureus* COL *hlb* promoter and open reading frame from SACOL_RS10470 (-355 from ATG start
288 codon and +40 after TAG stop codon) was cloned in EcoRI and SmaI sites of modified pAW8 (66).
289 The primers pairs used for the PCR are 5'-TTGCCGGAATTCTGCAACTTAATTATAGCCAGACTTTC-3'
290 and 5'-CATCAACCCGGGCGTCCTTTTAGAACGAAGCAAG-3'. Genomic co-ordinates of the 1388 bp
291 cloned segment are 2063371-2064758, as present on plasmid phlb.

292 **Construction of *fakB1*-repaired strain.** The *fakB1* gene of *S. aureus* RN450, as the entire NCTC
293 8325 lineage, displays a 483-bp deletion removing 56% of the 867-bp functional gene (Fig. S6).
294 To repair this deletion, a 1,939-bp DNA fragment containing a functional *fakB1* was amplified as
295 described for other NCTC 8325 derivatives (65). The *fakB1*-repaired strain is designated as
296 RN450-R.

297 **Growth media and conditions.** Brain heart infusion (BHI) was the base medium for *S. aureus*
298 cultures unless specified. Cultures were grown aerobically at 37°C and the starting $OD_{600nm}$ was
299 0.02 from a preculture at $OD_{600nm}$ between 1 and 5. Mouse serum (Clinisciences, France) was
300 added at 10% final concentration. Stocks of trilinolein (TNL, 50 mM), 1,2-dilinoleoylglycerol
301 (1.2DG, 50 mM), 1,3-dilinoleoylglycerol (1.3DG, 50 mM), palmitic acid (C16, 100 mM) (Larodan
302 Fine Chemicals, Sweden) and orlistat (38 mM, MedChemExpress, France) were prepared in
303 DMSO. Stocks of the anti-FabI antibiotic AFN-1252 (MedChemExpress, France) were prepared in
304 DMSO (1 mg/ml), and used at a final concentration of 0.5 µg/ml. To follow *S. aureus* adaptation
305 to AFN-1252, overnight cultures in BHI medium containing 10% mouse serum (Eurobio, France)
306 were inoculated in the same medium containing AFN-1252. $OD_{600}$ values were determined over
307 a 12 hour period.

308 **Determination of *S. aureus* fatty acid profiles.** FA profiles were performed as described (10). For
309 each condition, profiles were determined from three independent cultures. In these experiments
310 culture aliquots were routinely taken under exponential growth at $OD_{600}$ between 0.5 and 2.
311 After sample preparation (10), analyses were performed in a split-splitless injection mode on an
312 AutoSystem XL Gas Chromatograph (Perkin-Elmer) equipped with a ZB-Wax capillary column (30
313 m x 0.25 mm x 0.25 mm; Phenomenex, France). Data were recorded and analyzed by TotalChrom
314 Workstation (Perkin-Elmer). FA peaks were detected between 12 and 40 min of elution, and
315 identified by comparing to retention times of purified esterified FA standards (Mixture ME100,
316 Larodan, Sweden). Results are shown as representative gas chromatograph profiles, or as percent
317 of specific FA as calculated from their proportions compared to total peak areas (TotalChrom
318 Workstation; Perkin Elmer).

319 **Statistics analysis.** Graphs were prepared using Microsoft Excel software. Means and standard
320 deviations are presented for culture growth ($OD_{600nm}$/h) and FA percentages. Statistical
321 significance was determined by unpaired, nonparametric Mann Whitney tests, as recommended
322 for small sample sizes.

323 **Acknowledgments:** We gratefully acknowledge funding from the following French granting
324 agencies: French Agence Nationale de la Recherche (StaphEscape project ANR-16-CE15-0013),
325 and the Fondation pour la Recherche Medicale (DBF20161136769). We thank Myriam Gominet
326 (Institut Pasteur) for the construction of the *S. aureus* RN450 *fakB1*-repaired strain.

327

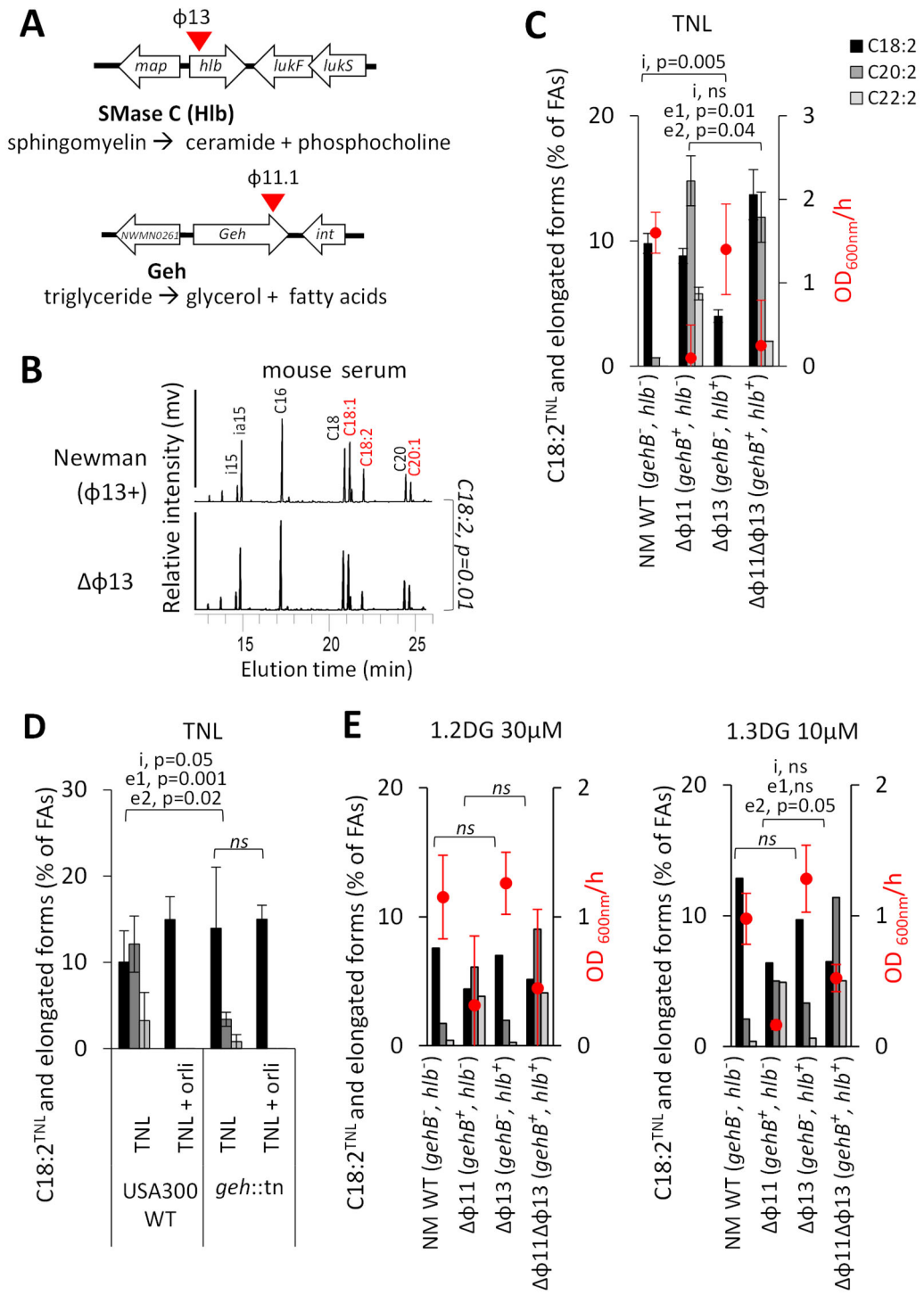


**FIG 1** *S. aureus* lysogenic status impacts incorporation and elongation of C18:2 derived from acylglycerides.

(*A*) Upper, site of ϕ13 insertion in *hlb*, encoding sphingomyelinase (Hlb). ϕ13 insertion results in enzyme N-terminal truncation (position 56 aa of the 330 aa protein). Lower, preferred site of ϕ11.1 insertion is *geh*, encoding triacylglycerol lipase (Geh). ϕ11-1 insertion results in truncation of the encoded triglyceride Geh (position 643 aa of the 690 aa protein).

(*B*) ϕ13 lysogen displays greater C18:2 incorporation from mouse serum than non-lysogen. The Newman strain (wild type, WT), a ϕ13 lysogen, and an isogenic Δϕ13 derivative were grown 2h in BHI medium containing 10% mouse serum. FA were extracted and analyzed by gas

338 chromatography. The y axis represents relative FA abundance (mV response) at indicated peak
339 positions. Black arrows indicate FA that can be endogenously produced. Red arrows indicate FA
340 not synthesized by *S. aureus* but incorporated from serum. Representative FA profiles from four
341 determinations are shown.
342 (*C*) ϕ13 and ϕ11 prophages interfere to modulate C18:2 incorporation and elongation from
343 trilinolein. Four isogenic Newman strains (NM) vary in prophage content, including ϕ11.1 and
344 ϕ13 (19). These isogenic strains were grown 2h in BHI medium supplemented with 30µM
345 trilinolein (comprising 3 oleic acid moieties). Growth is presented as the absorbance increase in
346 one hour ($OD_{600nm}$/h). Proportions of C18:2 and elongated forms (C20:2 and C22:2) were
347 determined from the FA profiles as in (*A*) and presented as percent of the total FA areas for each
348 profile (n=5).
349 (*D*) *geh* truncation decreases both incorporation and elongation of C18:2 from trilinolein. C18:2
350 incorporation from trilinolein is favored when *geh* is intact. USA300 ($geh^+$) and the *geh*::tn, were
351 grown in media supplemented with TNL. The Geh inhibitor orlistat (orli; 30 µM) was added as
352 indicated. The confirmed *geh*::tn mutant has a C-terminal truncated Geh (position 517 aa/690aa).
353 The percent of C18:2 and its elongated forms were determined as in (B). The OD/h of the *geh*::tn
354 mutant and the wild type were comparable (0.8 ± 0.3 for both cultures), (n=3).
355 (*E*) Acylated positions in a diglyceride determine C18:2 incorporation into *S. aureus* membrane
356 phospholipids**.** The four isogenic Newman strains, which differ in ϕ11.1 and ϕ13 prophages (19)
357 were grown 2h in BHI medium supplemented with 30 µM diglycerides comprising linoleic acid
358 moieties; 1,2-dilinoleoylglycerol (1.2DG) or 10µM 1,3-dilinoleoylglycerol (1.3DG), (n=4). Note
359 that 1.3DG was more incorporated and more toxic than 1.2DG; 30µM 1.3DG generated cell lysis
360 and FA profiles of unrepresentative non-lysed subpopulation (not shown). Studies were
361 therefore with 10µM. Percent of C18:2 and its elongated forms were determined as in (*B*). FA
362 profiles and percent of C18:2 and elongated forms are described as in (*B*).
363 p-values were determined by Mann Whitney test on percent total incorporated C18:2, including
364 elongated forms ('i'), and on percent elongation of C18:2 ('e1'), and C20:2 ('e2'); n.s., not
365 significant.
366

367
368
369
370
371

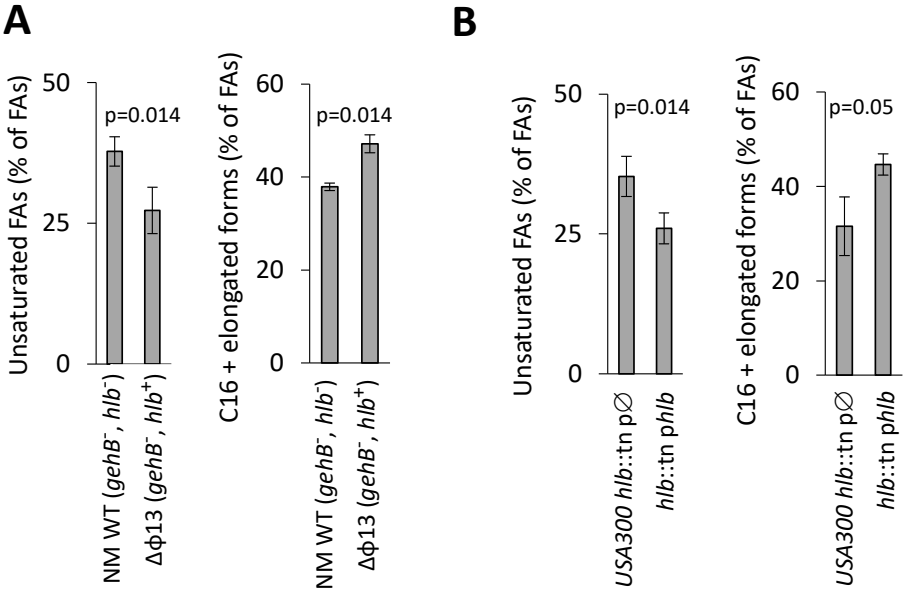


372
373
374
375
376

377 **FIG 2** Intact *hlb* favors incorporation of saturated FA and decreases incorporation of UFA from
378 serum. (*A*) Newman (NM) WT and Δϕ13 cultures were grown for 2 hours in BHI medium
379 supplemented with 10% mouse serum. The proportion of UFA (left) and SFA (right) are shown.
380 ϕ13 lysogeny increases unsaturated FA while lowering incorporation of C16 and elongated forms.
381 (*B*) Plasmid-driven expression of *hlb* increases incorporation of C16 and elongated forms, while
382 lowering incorporation of unsaturated FA. Cultures of the USA300 (USA) *hlb*::tn p∅ strain bearing
383 an empty plasmid or a plasmid carrying intact *hlb* (pHlb, derived from the COL strain) were grown
384 for 2.5 h in BHI supplemented with 10% mouse serum. FA extractions were performed and FA
385 profiles and area of FA were determined as in Fig. 1. Proportions of saturated FA (C16, C18and
386 C20) and unsaturated FA (C18:1Δ9, C18:1Δ11, C18:2 and C20:1) were compared to total FA
387 (shown as percent of total). Data presented are means ± standard deviations from three
388 independent experiments. p-values were determined by Mann Whitney test.
389

390
391
392
393
394
395

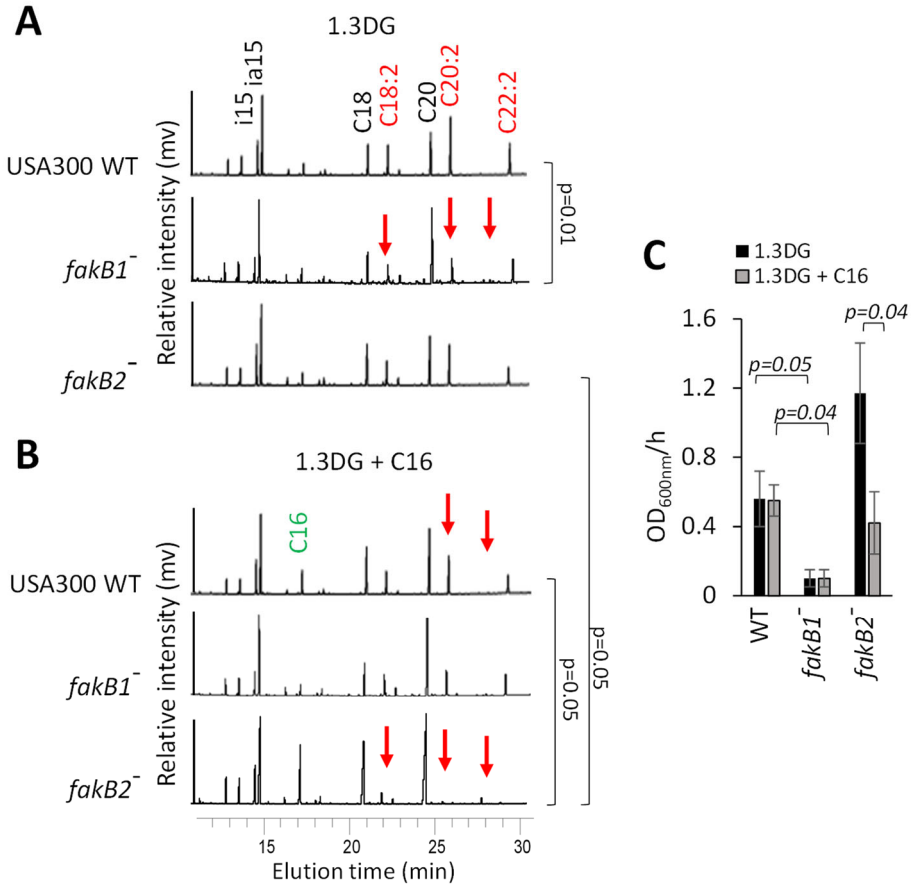


396
397
398
399
400
401 **FIG 3** *fakB1* and C16 modulate 1.3DG-derived C18:2 incorporation and its toxicity on growth. (*A*)
402 Involvement of *S. aureus fakB1* in 1.3DG-mediated C18:2 incorporation. USA300, *fakB1* and *fakB2*
403 strains were grown 2 hours in BHI supplemented with 10µM 1.3DG. (*B*) 1.3DG-derived C18:2 and
404 C16 compete for FakB1. Effects of C16 (20 µM) addition on C18:2 incorporation from 1.3DG were
405 assessed in USA300, *fakB1*, and *fakB2* strains, as in (*A*). Representative FA profiles are shown in
406 (A) and (B), (n=5). (*C*) Growth of WT and *fakB* mutants under conditions described in (*A*) and (*B*),
407 presented as $OD_{600nm}$ per hour. Representative profiles (*A*, *B*) or means (*C*) from four independent
408 experiments are presented. p-values were determined by Mann Whitney test for percent
409 incorporated C18:2, including elongated forms and OD/h.
410

411
412
413
414
415
416
417
418

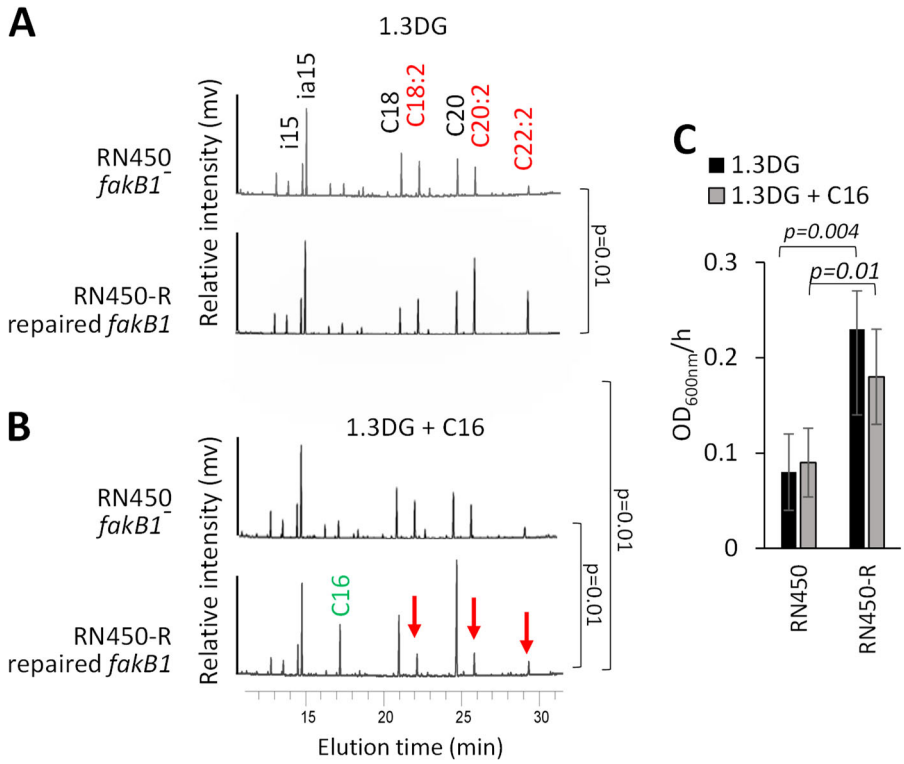


419
420
421
422
423
424 **FIG 4** Competition between 1.3DG-derived C18:2 and C16 at *fakb1* shapes incorporation into
425 phospholipid. (*A*) FA profiles of RN450 (*fakB1*$^{-}$) and RN450-R (*fakB1*$^{+}$) grown 2.5 h in BHI
426 supplemented with 10µM 1.3DG without or with 40µM C16. (*B*) Growth of RN450 and RN450-R
427 cultures from (*A*). Data presented are representative profiles (A) or means (C) from five
428 independent experiments. p-values were determined by the Mann Whitney test for percent
429 incorporated C18:2 (*A*)(including elongated forms) and OD/h (*B*).
430

431

432

433

434

435

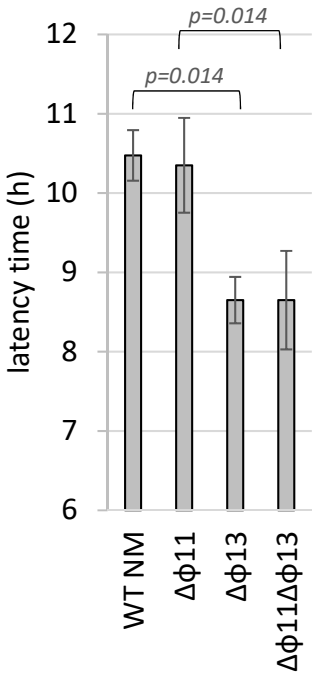


436

437

438 **FIG 5 ϕ13 prophage lows *S. aureus* adaptation to the FASII antibiotic AFN-1252.** The four
439 isogenic Newman strains (NM) vary in prophage content by the absence or presence of ϕ11.1
440 and ϕ13, as indicated. Strains were grown in BHI medium supplemented with 10% mouse serum
441 containing AFN-1252 (0.5µg/ml). Kinetic of anti-FASII adaptation was followed by $OD_{600}$
442 measurements. *S. aureus* undergoes a transient latency phase prior to outgrowth in AFN1252.
443 The latency time reduced in ϕ13 lysogens. Data presented are means from four independent
444 experiments. p-values were determined by the Mann Whitney test for latency times and were
445 significant ($p<0.05$) between ϕ13 lysogens and Δ ϕ13 strains.
446

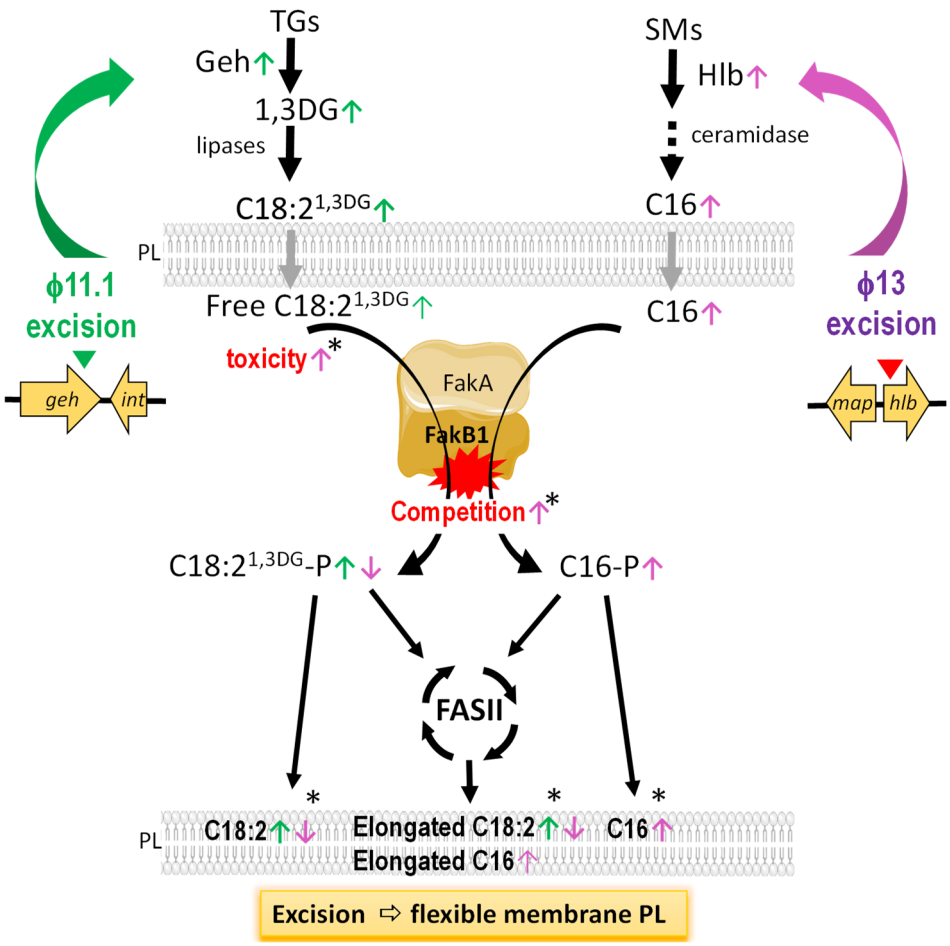


**FIG 6** A mechanistic model for environmental lipid utilization by *S. aureus*; ϕ11.1, ϕ13 and *fakB1* are lipid toxicity and membrane flexibility checkpoints.

ϕ11.1 lysogeny protects *S. aureus* from toxic C18:2 incorporation from triglyceride. ϕ11.1 in *geh* prevents TG hydrolysis, so that *S. aureus* incorporates low amounts of C18:2. In the absence of ϕ11.1, or upon stress-induced excision, intact Geh allows TG hydrolysis to 1.3 DG which promotes C18:2 incorporation. 1.3DG-derived C18:2 ($C18:2^{1.3DG}$) is incorporated via the FakA-FakB kinase system and the phosphorylated product ($C18:2^{1.3DG}$-P) may then be incorporated in phospholipids or cycled towards FASII for rounds of elongation before incorporation. The latter pathway is favored by intact Geh by an unknown mechanism.

FakB1 binds $C18:2^{1.3DG}$ and protects from its toxicity. Exogenous FA are phosphorylated *via* FakAB system comprising FakA kinase and FakB1 or FakB2 acyl binding proteins, initially reported as being specialized in saturated and unsaturated FA respectively (15, 17). Despite this bias, we showed in this study that C18:2 from TG or 1.3DG interacts with FakB1 binding protein.

Intact *hlb* interferes with binding of $C18:2^{1.3DG}$ to FakB1, with consequences on toxicity. The absence of ϕ13 (or oxidative stress condition) enables Hlb activity and liberation of C16 from serum SMs. This C16 competes with $C18:2^{1.3DG}$ for FakB1 binding and increases pools of free C18:2, which may be toxic. In contrast, ϕ13 lysogeny inactivates *hlb* and prevent sphingomyelins (SMs) hydrolysis, thus reducing competition. The entry of $C18:2^{1.3DG}$ via FakB1 may prevent

469 intracellular toxicity and lead to FA elongation via FASII. ϕ13 lysogeny thus fine-tunes membrane
470 flexibility via both C18:2$^{1.3DG}$ incorporation and elongation.
471 C18:2$^{1.3DG}$ represents C18:2 issued from 1.3DG. Impact of ϕ11.1, green arrows; impact of ϕ13,
472 purple arrows; unknown mechanism of fatty acid diffusion, gray arrows. Experimental results of
473 this study are indicated by the star (*).
474 **Supplementary information titles and legends**

475 **Supplementary FIG S1** ϕ11.1 or ϕ13 lysogeny has no effect on fatty acid (FA) profiles of *S. aureus*
476 grown in BHI medium. Four isogenic Newman strains, lysogenized or not by ϕ11.1 and ϕ13
477 prophages (1) were grown in BHI medium. FA were extracted at $OD_{600}$ = 1 and analyzed by gas
478 chromatography as described in material and methods. Representative FA profiles from three
479 determinations are shown.
480
481 **Supplementary FIG S2** Validation of free fatty acids (FA) incorporation in USA300 (WT), and *fakA,*
482 *fakB1* and *fakB2* mutant derivatives. The indicated strains were grown in BHI in the presence of
483 0.17 mM each free FA, C14:0, C16:0, and C18:1. FA were extracted and analyzed as in Fig. S1. The
484 three exogenous FA and elongated forms are indicated in red. Data presented are representative
485 profiles from three independent experiments.
486
487 **Supplementary FIG S3** Incorporation of free C18:2 in the *fakB2* mutant without and with C16
488 supplementation. The *fakB2* mutant was grown in BHI in the presence 10µM free C18:2 without
489 or with 40 µM C16, and fatty acids (FA) were extracted and analyzed as in Fig. S1. C16 in upper
490 panel corresponds to endogenous synthesis; the higher C16 peak in lower panel reflects
491 exogenous FA addition. Exogenous FA or their elongated forms are represented in red. Data
492 presented are representative profiles from three independent experiments.
493
494 **Supplementary FIG S4** *fakB1* and *fakB2* mutants both mediate C18:2 incorporation from
495 trilinolein, but only the *fakB2* mutant is affected by C16 addition. (*A*) C18:2 incorporation from
496 trilinolein in USA300 wild type and *fakB* mutants. Strains were grown two hours in BHI
497 supplemented with 30µM trilinolein, and fatty acid (FA) profiles were determined as in Fig. S1.
498 The y-axis represents relative fatty acid (FA) abundance (mV response). Exogenous FA
499 incorporated products (C18:2, C20:2, and C22:2) are in red. (B) Cultures were prepared as in (A),
500 except that 20 µM C16 was further added to medium. The *fakB2* mutant, which expresses FakB1,
501 is totally inhibited for C18:2 incorporation. Green and red arrows indicate changes due to C16
502 addition on peaks of C16, and C18:2 + elongated products, respectively. (C) Growth of WT, *fakB1*
503 and *fakB2* strains in the presence of trilinolein supplemented or not with C16. Samples
504 correspond to those presented in (*A*) and (*B*); results are presented as $OD_{600nm}$ per hour. Data
505 are representative profiles, (*A* and *B*) or means (*C*) from three independent experiments.
506
507 **Supplementary FIG S5** *fakB2*, and not *fakB1*, affects C18:2 incorporation from 1,2-
508 dilinoleoylglycerol (1.2DG). C18:2 incorporation from 1.2DG was assessed in USA300 WT, *fakB1*,
509 and *fakB2* strains. Strains were grown two hours in BHI supplemented with 30µM 1.2DG, and
510 fatty acids (FA) profiles were determined as in Fig. S1). Exogenous FA incorporated products
511 (C18:2, C20:2, and C22:2) are in red. The *fakB2* mutant shows significant inhibition of the
512 cumulative percentage of C18:2 and elongated forms (10 ± 3 %) compared to wild type (34 ± 5%).
513 Data are representative profiles from three independent experiments.
514

515 **Supplementary FIG S6** FakB1 defect in NCTC 8325 lineage, comprising RN450. Alignment of
516 FakB1 sequences from Newman (non-NCTC 8325 lineage) and NCTC 8325 strains. The non-
517 deleted region of NCTC 8325 FakB1 shares 99% identity with the synonymous region in
518 Newman. Red arrows indicate amino acids required for FA binding and for FakA-mediated
519 phosphotransfer (1).
520

521 **References**


522 1. Chen X, Alonzo F, 3rd. 2019. Bacterial lipolysis of immune-activating ligands promotes evasion of
523 innate defenses. Proc Natl Acad Sci USA 116:3764-3773
524 2. Gajenthra Kumar N, Contaifer D, Jr., Baker PR, Ekroos K, Jefferson KK, Wijesinghe DS. 2018.
525 Untargeted lipidomic analysis to broadly characterize the effects of pathogenic and non-
526 pathogenic staphylococci on mammalian lipids. PLoS One 13:e0206606.
527 3. Sun H, Zhang X, Shi W, Fang B. 2019. Association of soft tissue infection in the extremity with
528 glucose and lipid metabolism and inflammatory factors. Exp Ther Med 17:2535-2540.
529 4. Trinder M, Boyd JH, Brunham LR. 2019. Molecular regulation of plasma lipid levels during systemic
530 inflammation and sepsis. Curr Opin Lipidol 30:108-116.
531 5. Brinster S, Lamberet G, Staels B, Trieu-Cuot P, Gruss A, Poyart C. 2009. Type II fatty acid synthesis
532 is not a suitable antibiotic target for Gram-positive pathogens. Nature 458:83-6.
533 6. Brinster S, Lamberet G, Staels B, Trieu-Cuot P, Gruss A, Poyart C. 2010. Brief communication
534 arising replying to: W. Balemans *et al.* Nature 462, 10.1038/nature08667 (2009).
535 7. Gloux K, Guillemet M, Soler C, Morvan C, Halpern D, Pourcel C, Vu Thien H, Lamberet G, Gruss A.
536 2017. Clinical relevance of type II fatty acid synthesis bypass in *Staphylococcus aureus*. Antimicrob
537 Agents Chemother doi:10.1128/AAC.02515-16:61(5), e02515-16.
538 8. Hays C, Lambert C, Brinster S, Lamberet G, du Merle L, Gloux K, Gruss A, Poyart C, Fouet A. 2021.
539 Type II fatty acid synthesis pathway and cyclopropane ring formation are dispensable during
540 *Enterococcus faecalis* systemic infection. J Bacteriol 203:e0022121. doi 10.1128/JB.00221-21.
541 10.1128/JB.00221-21.
542 9. Kenanian G, Morvan C, Weckel A, Pathania A, Anba-Mondoloni J, Halpern D, Gaillard M, Solgadi
543 A, Dupont L, Henry C, Poyart C, Fouet A, Lamberet G, Gloux K, Gruss A. 2019. Permissive fatty fcid
544 Incorporation promotes staphylococcal adaptation to FASII antibiotics in host environments. Cell
545 Rep 29:3974-3982 e4.
546 10. Morvan C, Halpern D, Kenanian G, Hays C, Anba-Mondoloni J, Brinster S, Kennedy S, Trieu-Cuot P,
547 Poyart C, Lamberet G, Gloux K, Gruss A. 2016. Environmental fatty acids enable emergence of
548 infectious *Staphylococcus aureus* resistant to FASII-targeted antimicrobials. Nat Commun
549 7:12944.
550 11. Morvan C, Halpern D, Kenanian G, Pathania A, Anba-Mondoloni J, Lamberet G, Gruss A, Gloux K.
551 2017. The *Staphylococcus aureus* FASII bypass escape route from FASII inhibitors. Biochimie
552 141:40-46.
553 12. Feingold KR, Grunfeld C. 2000. The effect of inflammation and infection on lipids and lipoproteins.
554 *In* Feingold KR, Anawalt B, Boyce A, Chrousos G, Dungan K, Grossman A, Hershman JM, Kaltsas G,
555 Koch C, Kopp P, Korbonits M, McLachlan R, Morley JE, New M, Perreault L, Purnell J, Rebar R,
556 Singer F, Trence DL, Vinik A, Wilson DP (ed), Endotext, South Dartmouth (MA).
557 13. Kaysen GA, Ye X, Raimann JG, Wang Y, Topping A, Usvyat LA, Stuard S, Canaud B, van der Sande
558 FM, Kooman JP, Kotanko P, Monitoring Dialysis Outcomes I. 2018. Lipid levels are inversely
559 associated with infectious and all-cause mortality: international MONDO study results. J Lipid Res
560 59:1519-1528. 10.1194/jlr.P084277.
561 14. Delekta PC, Shook JC, Lydic TA, Mulks MH, Hammer ND. 2018. *Staphylococcus aureus* utilizes host-
562 derived lipoprotein particles as sources of fatty acids. J Bacteriol 200:(11):e00728-17.
563 15. Broussard TC, Miller DJ, Jackson P, Nourse A, White SW, Rock CO. 2016. Biochemical roles for
564 conserved residues in the bacterial fatty acid-binding protein family. J Biol Chem 291:6292-303.
565 16. Cuypers MG, Subramanian C, Gullett JM, Frank MW, White SW, Rock CO. 2019. Acyl-chain
566 selectivity and physiological roles of *Staphylococcus aureus* fatty acid-binding proteins. J Biol
567 Chem 294:38-49.
568 17. Parsons JB, Broussard TC, Bose JL, Rosch JW, Jackson P, Subramanian C, Rock CO. 2014.
569 Identification of a two-component fatty acid kinase responsible for host fatty acid incorporation
570 by *Staphylococcus aureus*. Proc Natl Acad Sci U S A 111:10532-7.

571 18. Arsic B, Zhu Y, Heinrichs DE, McGavin MJ. 2012. Induction of the staphylococcal proteolytic
572 cascade by antimicrobial fatty acids in community acquired methicillin resistant *Staphylococcus*
573 *aureus*. PLoS One 7:e45952.
574 19. Bae T, Baba T, Hiramatsu K, Schneewind O. 2006. Prophages of *Staphylococcus aureus* Newman
575 and their contribution to virulence. Mol Microbiol 62:1035-47.
576 20. Bosch M, Sanchez-Alvarez M, Fajardo A, Kapetanovic R, Steiner B, Dutra F, Moreira L, Lopez JA,
577 Campo R, Mari M, Morales-Paytuvi F, Tort O, Gubern A, Templin RM, Curson JEB, Martel N, Catala
578 C, Lozano F, Tebar F, Enrich C, Vazquez J, Del Pozo MA, Sweet MJ, Bozza PT, Gross SP, Parton RG,
579 Pol A. 2020. Mammalian lipid droplets are innate immune hubs integrating cell metabolism and
580 host defense. Science 370, aay8085.
581 21. Hines KM, Alvarado G, Chen X, Gatto C, Pokorny A, Alonzo F, 3rd, Wilkinson BJ, Xu L. 2020.
582 Lipidomic and ultrastructural characterization of the cell envelope of *Staphylococcus aureus*
583 grown in the presence of human serum. mSphere 5. doi 10.1128/mSphere.00339-20.
584 22. Nguyen MT, Hanzelmann D, Hartner T, Peschel A, Gotz F. 2016. Skin-specific unsaturated fatty
585 acids boost the *Staphylococcus aureus* innate immune response. Infect Immun 84:205-15.
586 23. Ubeda C, Maiques E, Knecht E, Lasa I, Novick RP, Penades JR. 2005. Antibiotic-induced SOS
587 response promotes horizontal dissemination of pathogenicity island-encoded virulence factors in
588 staphylococci. Mol Microbiol 56:836-44.
589 24. Goerke C, Pantucek R, Holtfreter S, Schulte B, Zink M, Grumann D, Broker BM, Doskar J, Wolz C.
590 2009. Diversity of prophages in dominant *Staphylococcus aureus* clonal lineages. J Bacteriol
591 191:3462-8.
592 25. Lee CY, Iandolo JJ. 1985. Mechanism of bacteriophage conversion of lipase activity in
593 *Staphylococcus aureus*. J Bacteriol 164:288-93.
594 26. Goerke C, Koller J, Wolz C. 2006. Ciprofloxacin and trimethoprim cause phage induction and
595 virulence modulation in *Staphylococcus aureus*. Antimicrob Agents Chemother 50:171-7.
596 27. Goerke C, Wirtz C, Fluckiger U, Wolz C. 2006. Extensive phage dynamics in Staphylococcus aureus
597 contributes to adaptation to the human host during infection. Mol Microbiol 61:1673-85.
598 28. Jung P, Abdelbary MM, Kraushaar B, Fetsch A, Geisel J, Herrmann M, Witte W, Cuny C, Bischoff
599 M. 2017. Impact of bacteriophage Saint3 carriage on the immune evasion capacity and hemolytic
600 potential of *Staphylococcus aureus* CC398. Vet Microbiol 200:46-51.
601 29. Salgado-Pabon W, Herrera A, Vu BG, Stach CS, Merriman JA, Spaulding AR, Schlievert PM. 2014.
602 *Staphylococcus aureus* beta-toxin production is common in strains with the beta-toxin gene
603 inactivated by bacteriophage. J Infect Dis 210:784-92.
604 30. Tang Y, Nielsen LN, Hvitved A, Haaber JK, Wirtz C, Andersen PS, Larsen J, Wolz C, Ingmer H. 2017.
605 Commercial Biocides Induce Transfer of Prophage Phi13 from Human Strains of *Staphylococcus*
606 *aureus* to Livestock CC398. Front Microbiol 8:2418.
607 31. Tran PM, Feiss M, Kinney KJ, Salgado-Pabon W. 2019. phiSa3mw prophage as a molecular
608 regulatory switch of *Staphylococcus aureus* beta-toxin production. J Bacteriol 201:e00766-18.
609 32. Parsons JB, Frank MW, Jackson P, Subramanian C, Rock CO. 2014. Incorporation of extracellular
610 fatty acids by a fatty acid kinase-dependent pathway in *Staphylococcus aureus*. Mol Microbiol
611 92:234-45.
612 33. Cadieux B, Vijayakumaran V, Bernards MA, McGavin MJ, Heinrichs DE. 2014. Role of lipase from
613 community-associated methicillin-resistant *Staphylococcus aureus* strain USA300 in hydrolyzing
614 triglycerides into growth-inhibitory free fatty acids. J Bacteriol 196:4044-56.
615 34. Zheng CJ, Yoo JS, Lee TG, Cho HY, Kim YH, Kim WG. 2005. Fatty acid synthesis is a target for
616 antibacterial activity of unsaturated fatty acids. FEBS Lett 579:5157-62.
617 35. Kitadokoro K, Tanaka M, Hikima T, Okuno Y, Yamamoto M, Kamitani S. 2020. Crystal structure of
618 pathogenic *Staphylococcus aureus* lipase complex with the anti-obesity drug orlistat. Sci Rep
619 10:5469.
620 36. Ikeda I, Yoshida H, Tomooka M, Yosef A, Imaizumi K, Tsuji H, Seto A. 1998. Effects of long-term
621 feeding of marine oils with different positional distribution of eicosapentaenoic and

622 docosahexaenoic acids on lipid metabolism, eicosanoid production, and platelet aggregation in
623 hypercholesterolemic rats. Lipids 33:897-904.
624 37. Schuhmacher M, Grasskamp AT, Barahtjan P, Wagner N, Lombardot B, Schuhmacher JS, Sala P,
625 Lohmann A, Henry I, Shevchenko A, Coskun U, Walter AM, Nadler A. 2020. Live-cell lipid
626 biochemistry reveals a role of diacylglycerol side-chain composition for cellular lipid dynamics and
627 protein affinities. Proc Natl Acad Sci U S A 117:7729-7738.
628 38. Yoshinaga K, Sasaki K, Watanabe H, Nagao K, Inoue N, Shirouchi B, Yanagita T, Nagai T, Mizobe H,
629 Kojima K, Beppu F, Gotoh N. 2015. Differential effects of triacylglycerol positional isomers
630 containing n-3 series highly unsaturated fatty acids on lipid metabolism in C57BL/6J mice. J Nutr
631 Biochem 26:57-63.
632 39. Douchet I, De Haas G, Verger R. 2003. Lipase regio- and stereoselectivities toward three
633 enantiomeric pairs of didecanoyl-deoxyamino-O methyl glycerol: a kinetic study by the
634 monomolecular film technique. Chirality 15:220-6.
635 40. Horchani H, Ben Salem N, Chaari A, Sayari A, Gargouri Y, Verger R. 2010. Staphylococcal lipases
636 stereoselectively hydrolyse the sn-2 position of monomolecular films of diglyceride analogs.
637 Application to sn-2 hydrolysis of triolein. J Colloid Interface Sci 347:301-8.
638 41. Lyberg AM, Adlercreutz P. 2008. Lipase specificity towards eicosapentaenoic acid and
639 docosahexaenoic acid depends on substrate structure. Biochim Biophys Acta 1784:343-50.
640 42. Hammad SM, Pierce JS, Soodavar F, Smith KJ, Al Gadban MM, Rembiesa B, Klein RL, Hannun YA,
641 Bielawski J, Bielawska A. 2010. Blood sphingolipidomics in healthy humans: impact of sample
642 collection methodology. J Lipid Res 51:3074-87.
643 43. Hanamatsu H, Ohnishi S, Sakai S, Yuyama K, Mitsutake S, Takeda H, Hashino S, Igarashi Y. 2014.
644 Altered levels of serum sphingomyelin and ceramide containing distinct acyl chains in young
645 obese adults. Nutr Diabetes 4:e141.
646 44. Kaplan N, Albert M, Awrey D, Bardouniotis E, Berman J, Clarke T, Dorsey M, Hafkin B, Ramnauth
647 J, Romanov V, Schmid MB, Thalakada R, Yethon J, Pauls HW. 2012. Mode of action, in vitro activity,
648 and in vivo efficacy of AFN-1252, a selective antistaphylococcal FabI inhibitor. Antimicrob Agents
649 Chemother 56:5865-74. 10.1128/AAC.01411-12.
650 45. Butcher GW, King G, Dyke KG. 1976. Sensitivity of *Staphylococcus aureus* to unsaturated fatty
651 acids. J Gen Microbiol 94:290-6.
652 46. Desbois AP, Smith VJ. 2010. Antibacterial free fatty acids: activities, mechanisms of action and
653 biotechnological potential. Appl Microbiol Biotechnol 85:1629-42.
654 47. Kabara JJ, Swieczkowski DM, Conley AJ, Truant JP. 1972. Fatty acids and derivatives as
655 antimicrobial agents. Antimicrob Agents Chemother 2:23-8.
656 48. Kelsey JA, Bayles KW, Shafii B, McGuire MA. 2006. Fatty acids and monoacylglycerols inhibit
657 growth of *Staphylococcus aureus*. Lipids 41:951-61.
658 49. Knapp HR, Melly MA. 1986. Bactericidal effects of polyunsaturated fatty acids. J Infect Dis 154:84-
659 94.
660 50. Zhang Q, Wu W, Zhang J, Xia X. 2020. Antimicrobial lipids in nano-carriers for antibacterial
661 delivery. J Drug Target 28:271-281.
662 51. Krute CN, Ridder MJ, Seawell NA, Bose JL. 2019. Inactivation of the exogenous fatty acid utilization
663 pathway leads to increased resistance to unsaturated fatty acids in *Staphylococcus aureus*.
664 Microbiology 165:197-207.
665 52. Alnaseri H, Kuiack RC, Ferguson KA, Schneider JET, Heinrichs DE, McGavin MJ. 2019. DNA binding
666 and sensor specificity of FarR, a novel TetR family regulator required for induction of the fatty scid
667 efflux pump FarE in *Staphylococcus aureus*. J Bacteriol 201.
668 53. Deutsch DR, Utter B, Verratti KJ, Sichtig H, Tallon LJ, Fischetti VA. 2018. Extra-chromosomal DNA
669 sequencing reveals episomal prophages capable of impacting virulence factor expression in
670 *Staphylococcus aureus*. Front Microbiol 9:1406.
671 54. Al-Daghri NM, Torretta E, Barbacini P, Asare H, Ricci C, Capitanio D, Guerini FR, Sabico SB, Alokail
672 MS, Clerici M, Gelfi C. 2019. Sphingolipid serum profiling in vitamin D deficient and dyslipidemic
673 obese dimorphic adults. Sci Rep 9:16664.

674 55. Astorg P, Bertrais S, Laporte F, Arnault N, Estaquio C, Galan P, Favier A, Hercberg S. 2008. Plasma
675 n-6 and n-3 polyunsaturated fatty acids as biomarkers of their dietary intakes: a cross-sectional
676 study within a cohort of middle-aged French men and women. Eur J Clin Nutr 62:1155-61.
677 56. Dobner J, Kaser S. 2018. Body mass index and the risk of infection - from underweight to obesity.
678 Clin Microbiol Infect 24:24-28.
679 57. Hodson L, Skeaff CM, Fielding BA. 2008. Fatty acid composition of adipose tissue and blood in
680 humans and its use as a biomarker of dietary intake. Prog Lipid Res 47:348-80.
681 58. Trinder M, Walley KR, Boyd JH, Brunham LR. 2020. Causal inference for genetically determined
682 levels of high-density lipoprotein cholesterol and risk of infectious disease. Arterioscler Thromb
683 Vasc Biol 40:267-278.
684 59. Lopez MS, Tan IS, Yan D, Kang J, McCreary M, Modrusan Z, Austin CD, Xu M, Brown EJ. 2017. Host-
685 derived fatty acids activate type VII secretion in *Staphylococcus aureus*. Proc Natl Acad Sci U S A
686 114:11223-11228.
687 60. Nguyen MT, Luqman A, Bitschar K, Hertlein T, Dick J, Ohlsen K, Broker B, Schittek B, Gotz F. 2018.
688 Staphylococcal (phospho)lipases promote biofilm formation and host cell invasion. Int J Med
689 Microbiol 308:653-663.
690 61. Jimenez-Dalmaroni MJ, Radcliffe CM, Harvey DJ, Wormald MR, Verdino P, Ainge GD, Larsen DS,
691 Painter GF, Ulevitch R, Beutler B, Rudd PM, Dwek RA, Wilson IA. 2015. Soluble human TLR2
692 ectodomain binds diacylglycerol from microbial lipopeptides and glycolipids. Innate Immun
693 21:175-93.
694 62. Rohmer C, Wolz C. 2021. The role of *hlb*-converting bacteriophages in *Staphylococcus aureus* host
695 adaption. Microb Physiol 31:109-122.
696 63. Fey PD, Endres JL, Yajjala VK, Widhelm TJ, Boissy RJ, Bose JL, Bayles KW. 2013. A genetic resource
697 for rapid and comprehensive phenotype screening of nonessential *Staphylococcus aureus* genes.
698 mBio 4:e00537-12.
699 64. Herbert S, Ziebandt AK, Ohlsen K, Schafer T, Hecker M, Albrecht D, Novick R, Gotz F. 2010. Repair
700 of global regulators in *Staphylococcus aureus* 8325 and comparative analysis with other clinical
701 isolates. Infect Immun 78:2877-89.
702 65. Pathania A, Anba-Mondoloni J, Gominet M, Halpern D, Dairou J, Dupont L, Lamberet G, Trieu-Cuot
703 P, Gloux K, Gruss A. 2021. (p)ppGpp/GTP and malonyl-CoA modulate *Staphylococcus aureus*
704 adaptation to FASII antibiotics and provide a basis for synergistic bi-therapy. mBio 12:e03193-20.
705 doi 10.1128/mBio.03193-20.
706 66. Katayama Y, Zhang HZ, Hong D, Chambers HF. 2003. Jumping the barrier to beta-lactam resistance
707 in *Staphylococcus aureus*. J Bacteriol 185:5465-72.
708